1521-0111/91/4/287–295$25.00
MOLECULAR PHARMACOLOGY

http://dx.doi.org/10.1124/mol.116.106526
Mol Pharmacol 91:287–295, April 2017

# Targeting a Proteinase-Activated Receptor 4 (PAR4) Carboxyl Terminal Motif to Regulate Platelet Function[S]

Rithwik Ramachandran, Koichiro Mihara, Pierre Thibeault, Christina M. Vanderboor, Björn Petri, Mahmoud Saifeddine, Michel Bouvier, and Morley D. Hollenberg

*Snyder Institute for Chronic Diseases and Department of Physiology and Pharmacology (R.R., K.M., M.S., M.D.H.), Mouse Phenomics Resource Laboratory, Snyder Institute for Chronic Diseases and Department of Microbiology, Immunology, and Infectious Diseases (B.P.), and Department of Medicine (M.D.H.), Cumming School of Medicine, University of Calgary, Calgary, Alberta, Canada; Department of Physiology and Pharmacology, Schulich School of Medicine and Dentistry, University of Western Ontario, London, Ontario, Canada (R.R., P.T., C.M.V.); and IRIC-Université de Montréal, Montréal, Québec, Canada (M.B.)*

Received August 24, 2016; accepted January 18, 2017

## ABSTRACT

Thrombin initiates human platelet aggregation by coordinately activating proteinase-activated receptors (PARs) 1 and 4. However, targeting PAR1 with an orthosteric-tethered ligand binding-site antagonist results in bleeding, possibly owing to the important role of PAR1 activation on cells other than platelets. Because of its more restricted tissue expression profile, we have therefore turned to PAR4 as an antiplatelet target. We have identified an intracellular PAR4 C-terminal motif that regulates calcium signaling and $\beta$-arrestin interactions. By disrupting this PAR4 calcium/$\beta$-arrestin signaling process with a novel cell-penetrating peptide, we were able to inhibit both thrombin-triggered platelet aggregation in vitro and clot consolidation in vivo. We suggest that targeting PAR4 represents an attractive alternative to blocking PAR1 for antiplatelet therapy in humans.

## Introduction

Platelet activation and the formation of a multiplatelet thrombus subsequent to blood vessel injury underlie the pathophysiology of a number of cardiovascular diseases. Therapeutic intervention to prevent thrombosis involves the use of anticoagulants or antiplatelet agents. Anticoagulants include direct coagulation pathway inhibitors (coumarins, heparins, and thrombin catalytic site inhibitors). Although clinically effective, these agents present with significant challenges and require stringent patient monitoring. Thus, much effort has been expended to develop antiplatelet agents, including the widely used salicylates, GPIIb/IIIa inhibitors, and ADP receptor antagonists. These agents are also clinically very useful and used widely; however, there are many drawbacks and side effects that limit their use (McKee et al., 2002; Wiviott and Antman, 2004).

Thrombin is the most potent activator of platelets, and in humans it acts on two G protein-coupled receptors (GPCRs), proteinase-activated receptors (PARs) 1 and 4 (Coughlin, 2000), to trigger multiple responses, including platelet shape change, granule secretion, and aggregation. These actions have prompted the search for drugs that target the thrombin-activated receptor, PAR1 (Bernatowicz et al., 1996; Andrade-Gordon et al., 1999; Chackalamannil et al., 2005; Serebruany et al., 2009). Thrombin activates PARs 1 and 4 by proteolytically unmasking an N-terminal motif that acts as a tethered ligand to initiate signaling. This tethered-ligand mechanism has made development of antagonists challenging. Notwithstanding, the small-molecule PAR1 peptidomimetic antagonists that have been developed (Derian et al., 2003; Chackalamannil et al., 2005, 2008) have resulted in clinically useful agents like vorapaxar (SCH530348; trade name Zontivity) (Goto et al., 2010; Morrow et al., 2012; Baker et al., 2014) that block thrombin-mediated platelet aggregation at the same time retaining thrombin's hemostatic clotting activity. Unfortunately, some unexpected side effects have become evident in the course of the clinical studies of vorapaxar, including incidences of intracranial bleeding (Morrow et al., 2009, 2012; Tricoci et al., 2012). Although not fully understood, one explanation for the bleeding diatheses could come from the relatively widespread expression of PAR1, particularly on endothelial cells (Ramachandran, 2012), where it has an important role in maintaining the integrity of the endothelial barrier (Feistritzer et al., 2006; Bae and Rezaie, 2008; Schuepbach et al., 2009). Endothelial barrier protective responses through PAR1 are triggered by activated protein C, as opposed to thrombin activation of PAR1, which can disrupt the endothelial barrier (Riewald and

This work was funded by grants from the Canadian Institutes of Health Research to R.R., M.D.H., and M.B.
dx.doi.org/10.1124/mol.116.106526.
[S] This article has supplemental material available at molpharm.aspetjournals.org.

**ABBREVIATIONS:** BRET, bioluminescence resonance energy transfer; eYFP, enhanced yellow fluorescent protein; GPCR, G protein-coupled receptors; HEK, human embryonic kidney–derived cells; ICL3, third intracellular loop; MAPK, mitogen-activated protein kinase; PAR, proteinase-activated receptor; PBS, phosphate-buffered saline; RAG8, palmitoyl-RAGLFQRS-$NH_2$; RLuc, Renilla luciferase; YFP, yellow fluorescent protein; wt, wild-type.

Ruf, 2005; Schuepbach et al., 2012). More recently, compounds that target PAR1 on the intracellular face of the receptor have been developed to target prothrombotic signaling specifically through this receptor, at the same time sparing the cytoprotective signaling pathways (Dowal et al., 2011; Aisiku et al., 2015). Thus, compounds that bind to the third intracellular loop of PAR1 inhibit $G\alpha_{13}$-dependent signaling (Aisiku et al., 2015), whereas compounds that interact with helix 8 of PAR1 block $G\alpha_q$-dependent signaling (Dowal et al., 2011).

Given the challenges in selectively blocking the detrimental effects of activating PAR1 on platelets and at the same time maintaining PAR1 cytoprotective responses in endothelial cells, we turned to the other platelet thrombin receptor—PAR4 (Xu et al., 1998). PAR4 has a more restricted tissue expression profile and could be a more tractable therapeutic target for antiplatelet therapy in humans. Our initial studies were aimed at understanding the intracellular receptor motifs regulating signal transduction through PAR4. We identified an intracellular C-terminal sequence in PAR4 that regulates calcium signaling and is critical for PAR4-$\beta$-arrestin interactions. We followed on with the development of a cell-penetrating peptide formed on the basis of that sequence that blocks PAR4 signaling and platelet aggregation in vitro and prevents clot consolidation in vivo.

## Materials and Methods

**Chemicals and Other Reagents.** Thrombin from human plasma (cat. no. 605195; 2800 NIH units/mg), verified to be free of trypsin-like activity using soya trypsin inhibitor, was from EMD Biosciences (San Diego, CA). A concentration of 1 unit/ml was calculated to be 10 nM thrombin.

**Design and Synthesis of Agonist and Antagonist Peptides.** All peptides, (>95% purity: HPLC/mass spectrum) were purchased from the Peptide Synthesis Facility, University of Calgary (peplab@ucalgary.ca) or EZBiolabs (Carmel, IN). The PAR4 antagonist targeting the C-terminal intracellular face of PAR, corresponding to the receptor's putative arrestin-interacting site, was prepared as an N-terminal palmitoylated peptide to facilitate its insertion into the plasma membrane. The antagonist peptide, palmitoyl-RAGLFQRS-$NH_2$ (RAG8) and the control reverse-sequence peptide, palmitoyl-SRQFLGAR-$NH_2$ (SRQ8:Reverse-RAG8) were custom synthesized by EZBiolabs using standard solid-phase synthesis, purified by reverse-phase high-performance liquid chromatography and verified by mass spectrometry analysis.

**Cell Lines and Culture Conditions.** All media and cell culture reagents were purchased from Thermo Fisher Scientific (Waltham, MA). Human embryonic kidney (HEK)–derived cells (HEK-293; ATCC) were maintained in Dulbecco's modified Eagle's medium supplemented with 10% fetal bovine serum, sodium pyruvate, and 2.5 $\mu$g/ml plasmocin (Invivogen, San Diego CA). Cells stably transfected with wild-type (wt) or mutated PAR4-expressing vectors were routinely cultured in the above media supplemented with 600 $\mu$g/ml G418. Since trypsin activates the PARs, cells were routinely subcultured using enzyme-free isotonic phosphate-buffered saline (PBS), pH 7.4, containing 1 mM EDTA and plated in appropriate culture plates or glass-bottom slides for further experimentation.

**Molecular Cloning and Constructs.** The plasmid encoding human PAR4 (wt-hPAR4) cloned in pCDNA3.1 (GenBank: AY431102.1) was obtained from the cDNA Resource Center (University of Missouri, Rolla, MO; currently hosted at Bloomsburg University, Bloomsburg, PA). A C-terminal enhanced yellow fluorescent protein (eYFP) tag was fused in-frame with the PAR4 sequence by mutating the PAR4 stop codon to tyrosine and inserting the eYFP fragment with flanking XhoI and XbaI restriction-enzyme sites at the C terminus of the PAR4 coding sequence. Plasmid DNA mutations in the C-terminus of PAR4 were created using the QuikChange Lightning Multi Site-Directed Mutagenesis Kit (Agilent Technologies, Mississauga, ON, Canada) to generate all mutants described in this study. All constructs were verified by direct sequencing (University of Calgary DNA sequencing facility). Cells were transfected with FuGENE 6 (Promega, Madison, WI) in six-well multiplates (Nunc; Sigma-Aldrich, St. Louis, MO). Transfected cells were subcultured under G418 (600 $\mu$g/ml) selection and sorted by flow cytometry, and cell stocks were maintained in liquid nitrogen for future experiments.

**Calcium Signaling.** Calcium signaling experiments were performed essentially as described before (Ramachandran et al., 2011; Mihara et al., 2013). Cells cultured to approximately 80% confluency in a T75 flask were detached in enzyme-free cell dissociation buffer, resuspended in 18 ml of serum-containing growth medium, and 100 $\mu$l/well of the cell suspension was plated in black-walled cell culture–treated clear-bottom 96-well plates (Corning, Corning, NY) and cultured overnight. The next day, adherent cells were washed with PBS and placed in 100 $\mu$l of Fluo-4-AM NW (no wash) calcium indicator dye (Thermo Fisher Scientific). Intracellular fluorescence (excitation 480 nm; emission recorded at 530 nm) was monitored for 2 minutes after the injection of agonists (enzymes or PAR-activating peptides) into each well, using a Victor $\times$4 plate reader (PerkinElmer, Waltham, MA). The increase in fluorescence emission monitored at 530 nm was used as an index of increases in intracellular calcium. In some experiments calcium signaling was also monitored in Fluo4-loaded cells in suspension using an AB2 Spectrofluorometer (Thermo Fisher Scientific). Where appropriate, responses were normalized to the calcium signal generated by 2 $\mu$M A23178 (Sigma-Aldrich), a calcium ionophore.

**Mitogen-Activated Protein Kinase Assay.** Agonist-stimulated mitogen-activated protein kinase (MAPK) signaling in HEK-293 cells expressing wt-PAR4-YFP or dRS-PAR4-YFP was monitored by Western blot analysis as described previously (Ramachandran et al., 2011; Mihara et al., 2013). In brief, cells were rinsed with PBS and placed in serum free media. Cells were then stimulated with agonists for varying time periods, rapidly rinsed with ice-cold isotonic PBS and placed on ice. Total protein was extracted by adding ice-cold lysis buffer (20 mM Tris-HCl, pH 7.5, 100 mM NaCl, 10 mM $MgCl_2$, 1 mM EDTA, 1 mM EGTA, 0.5% NP40, 2.5 mM sodium pyrophosphate, 1 mM $\beta$-glycerophosphate, 1 mM $Na_3VO_4$, 25 mM NaF, 1 $\mu$g/ml leupeptin, 1 $\mu$g/ml aprotinin, 1 mM phenylmethylsulfonyl fluoride, and 1mM dithiothreitol) and cleared by centrifugation (15,000*g* for 10 minutes). The protein samples were heat-denatured at 92°C for 10 minutes in denaturing Laemmli buffer and resolved on 4–20% gradient Novex Tris-Glycine Gels (Thermo Fisher Scientific). The resolved proteins were transferred to a polyvinylidene difluoride membrane blocked in PBST buffer [PBS with 0.1% (v/v) Tween-20] supplemented with 1% ECL Advance Blocking Agent (GE Healthcare, Waukesha, WI) for 1 hour at room temperature. p42/44 (Thr202/Tyr204), p38 (Thr180/Tyr182), and AKT (Ser 473) phosphorylation was detected with specific antibodies (Cell Signaling Technology, Danvers, MA) (diluted 1:2000 in PBST with 1% ECL Advance Blocking Agent) overnight at 4°C. phospho-P42/44 immunoreactivity was detected using the horseradish peroxidase-conjugated anti-mouse or -rabbit secondary antibody (Cell Signaling Technology) (1:10,000 in PBST/1% ECL Advance Blocking Agent for 1 hour). After washing the membrane with PBST, the peroxidase activity was detected with the chemiluminescence reagent ECL Advance (GE Healthcare) on a KODAK Image Station 4000MM (Kodak, Rochester, NY). Polyvinylidene difluoride membranes were then stripped with stripping buffer (Thermo Fisher Scientific) at room temperature and blocked in PBST with 1% ECL Advance Blocking Agent before incubation with the appropriate Total-P42/44 (t-P42/44), T-p38, or T-AKT antibody (1:2000 in PBST with 1% ECL Advance Blocking Agent) overnight at 4°C and incubation with the horseradish peroxidase -conjugated anti-rabbit secondary antibody (1:10,000 in PBST/1% ECL Advance Blocking Agent for 1 hour). Membranes were washed with PBST and imaged

using the chemiluminescence reagent (ECL Advance) and a Kodak Image Station 4000MM. Band intensities representing activated MAPK were quantified using the ImageJ quantification software (http://rsbweb.nih.gov.ezproxy.lib.ucalgary.ca/ij/). Phospho-kinase levels were normalized for differences in protein loading by expressing the data as a percentage of the corresponding total-kinase signal. MAPK activation was also monitored using the Proteome Profiler Human Phospho-MAPK Array ARY002 (R&D Systems, Minneapolis, MN) according to the manufacturer's instructions. Platelet AKT activation was monitored following extraction of proteins from 100 $\mu$l of a washed platelet suspension ($3 \times 10^8$ cells/ml, see below) using the same protein extraction and Western blotting procedures described above. Cell were stimulated with agonists for 10 minutes and all antagonist pretreatment was done for 20 minutes.

**Confocal Microscopy.** HEK-293 cells transfected with wt-PAR4-YFP or dRS-PAR4-YFP with FuGENE 6 in six-well plates were subcultured into 35-mm glass-bottom culture dishes (MatTek Corporation, Ashland, MA) and placed in growth medium for an additional 16 hours. Cells were stimulated with agonists for specified times, fixed with 10% buffered formalin, and receptor trafficking was monitored by imaging eYFP expression with an Olympus FV1000 confocal microscope system on an Olympus IX70 microscope using the FluoView system software (Melville, NY).

**Bioluminescence Resonance Energy Transfer Detection of $\beta$-Arrestin Recruitment.** Bioluminescence resonance energy transfer (BRET)–based detection of $\beta$-arrestin-1 and -2 interaction with wt-PAR4-YFP and dRS-PAR4-YFP was monitored in HEK-293 cells as described (Ramachandran et al., 2009, 2011). PAR-YFP (1 $\mu$g) and Renilla luciferase-tagged $\beta$-arrestin-1 (RLuc-$\beta$-arr1 and 2) (0.1 $\mu$g) were transiently transfected for 48 hours. Cells were plated in white 96-well culture plates (Brandplates; Brand, Essex, CT), and interactions between the receptors and $\beta$-arrestin-1/2 were detected by measuring BRET at timed intervals over 20 minutes following the addition of 5 $\mu$M coelenterazine (NanoLight Technology, Pinetop, AZ) on a Mithras fluorescence plate reader (Berthold Technologies, Bad Wildbad, Germany) in luminescence mode using the appropriate filters.

**Platelet Isolation and Aggregation Assay.** Blood was drawn under informed consent (REB14-0367) from healthy volunteers who denied taking any antiplatelet drugs by standard venipuncture into 4-ml Vacutainer tubes containing 0.45 ml of 0.1 M sodium citrate solution. Platelet aggregation studies were done with washed platelets. The blood was centrifuged at 300*g* for 15 minutes and the platelet-rich plasma was transferred to 50-ml conical tubes containing 10% acid citrate dextrose solution (39 mM citric acid, 75 mM sodium citrate, 135 mM glucose, pH 7.4). Following another centrifugation step at 800*g* the pelleted cells were resuspended in Tyrode's buffer (12 mM $NaHCO_3$, 127 mM NaCl, 5 mM KCl, 0.5 mM $NaH_2PO_4$, 1 mM $MgCl_2$, 5 mM glucose, and 10 mM HEPES), counted on a Coulter counter, and adjusted to a concentration of $3 \times 10^8$ cells/ml. 400 $\mu$l of this cell suspension was used for light transmission aggregometry on a platelet aggregometer (Chrono-Log Corp, Havertown, PA).

**Confocal Intravital Imaging In Vivo.** Mice (8- to 10-week-old male C57BL/6) were injected intraperitoneally with 20 mg/kg RAG8 or the control reverse-RAG8 in 100 $\mu$l of isotonic PBS, pH 7.4. Mice were then anesthetized (10 mg per kg body weight xylazine hydrochloride and 200 mg per kg body weight ketamine hydrochloride), and body temperature was maintained using a heating pad. The right jugular vein was cannulated to administer additional anesthetic and fluorescent labels. Platelets were labeled with a CD49b antibody coupled to Alexa 647 (5 $\mu$g/mouse; BioLegend, San Diego, CA) and blood vessels were labeled with an anti-CD31 (PECAM) antibody coupled to phycoerythrin (2 $\mu$g/mouse, Affymetrix/eBioscience; Thermo Fisher Scientific). The femoral artery and vein were surgically exposed, baseline readings were taken and a 1–2 $mm^2$ filter paper soaked in 10% $FeCl_3$ was placed on the blood vessels for 3 minutes. The injury site was rinsed thoroughly by perfusing with isotonic saline, and development of the thrombus was imaged using spinning disc confocal microscopy. Imaging was performed using an Olympus BX51W1 upright microscope equipped with a 4×/0.16UPlanSApo or 10×/0.30 UPlanFLN objective. The microscope was equipped with a confocal light path (WaveFx; Quorum Technologies, Guelph, ON, Canada) a modification of the Yokogawa CSU-10 head (Sugar Land, TX). Laser excitation at 488, 561, 649, and 730 nm (cobalt) was used in rapid succession, and fluorescence in green, red, and blue channels was visualized with the appropriate long-pass filters (Semrock, Rochester, NY). Exposure time for all wavelengths was constant at 1 second. Sensitivity settings were kept the same for all experiments. A 512 × 512 pixel back-thinned EMCCD camera (C9100-13; Hamamatsu, Hamamatsu City, Shizuoka, Japan) was used for fluorescence detection. Volocity Acquisition software (Improvision/PerkinElmer) was used to drive the confocal microscope. Images captured using the spinning disk were processed and analyzed in Volocity 4.20. Thrombus area was quantified over the entire field of view for each treatment using the Volocity software.

**Measurement of Tail-Vein Bleeding Times.** Mice were injected with 20 mg/kg RAG8 or control reverse-RAG8 and anesthetized with an intraperitoneal injection of ketamine/xylazine (10 mg per kg body weight xylazine hydrochloride and 200 mg per kg body weight ketamine hydrochloride). The tails were transected 0.5 cm from the tip and placed in a cuvette containing saline at 37°C. The time taken for the cessation of blood flow was monitored. Once blood flow had stopped, the vein was monitored for a further 60 seconds to confirm stable occlusion. If blood flow resumed within the 1-minute timeframe, the time taken for cessation of continued blood flow was monitored again up to 800 seconds.

**Statistical Analysis.** Statistical analysis of data and curve fitting were done with Prism 5 software (GraphPad Software, La Jolla, CA). Statistical significance was assessed using the Student's *t* test or analysis of variance with Tukey's post-test.

## Results

**Impaired Calcium Signaling via C-Terminal Mutant PAR4 Receptors.** On the basis of sequence alignment, we initially observed that human PAR4 lacked a cysteine residue that is present in the rodent PAR4 (C368 in mouse PAR4) C-terminus and in the human PAR1 (C387-388) and PAR2 (C361). Since C-terminal cysteine residues serve as sites of receptor palmitoylation and regulate signaling (Qanbar and Bouvier, 2003), we generated mutant PAR4 receptors QC-PAR4 in which the glutamine is mutated to a cysteine, as well as a variant which had an eight-amino acid deletion flanking this region (dRS-PAR4) (Table 1).

To examine the functional consequence of such mutations, HEK-293 cells transiently expressing wt-PAR4-YFP, QC-PAR4-YFP, and dRS-PAR4-YFP (Table 1; Fig. 1A) were loaded with Fluo-4 AM NW, and the calcium signaling triggered by the PAR4-selective activating peptide AYPGKF-$NH_2$ was monitored. Since HEK-293 cells do not endogenously express PAR4, the calcium signal detected originated entirely from the transfected constructs. Equal levels of cell-surface expression were observed for all constructs when transiently expressed at 48 hours, and we further generated cell lines permanently expressing equivalent levels of wt-PAR4-YFP and dRS-PAR4-YFP by flow

TABLE 1
Amino acid sequence of the human PAR4 C-terminus highlighting the different mutant constructs described in this study

| | |
|---|---|
| WT-PAR4-YFP | SAEFRDKVRAGLFQRSPGDTVASKASAE-YFP |
| QC-PAR4-YFP | SAEFRDKVRAGLF**C**RSPGDTVASKASAE-YFP |
| dRS-PAR4-YFP | SAEFRDKV————PGDTVASKASAE-YFP |

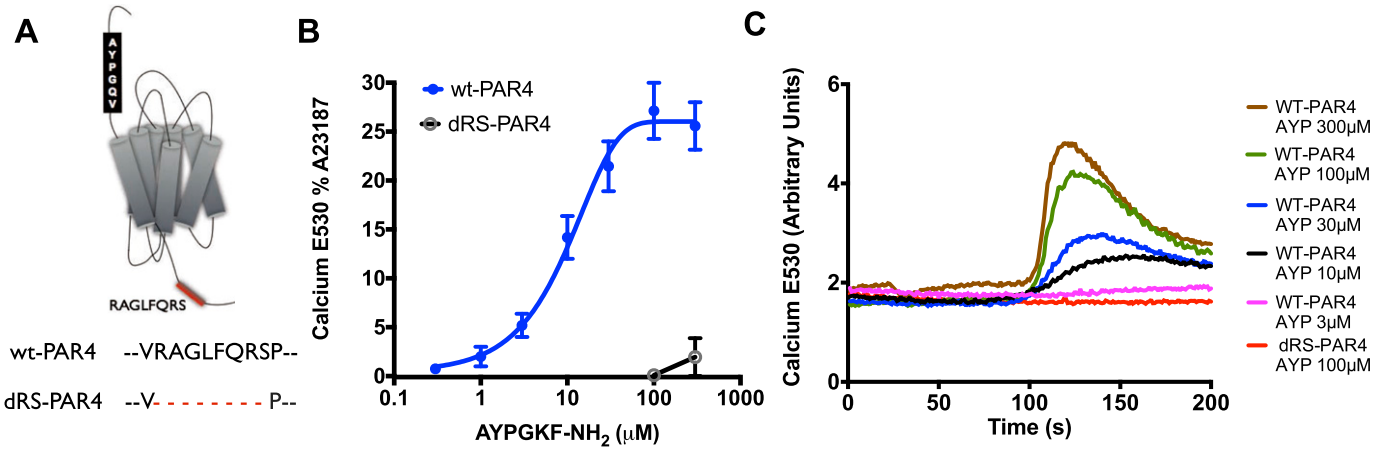


**Fig. 1.** PAR4 C-terminal domain regulates calcium signaling. (A) Scheme depicting the location and amino acid sequence for the PAR4 regulatory C-terminal motif. (B) In HEK cells transfected with wt-human PAR4 (wt-PAR4) or a PAR4 mutant with a deletion of the eight-amino acid motif (dRS-PAR4). Deletion of the C-terminal motif abolishes PAR4-dependent calcium signaling. Data are expressed as the mean data ± S.E.M. relative to calcium ionophore A23187 from at least three separate experiments. (C) Representative traces showing dose-dependent AYPGKF-$NH_2$–triggered calcium signaling in wt-PAR4-expressing cells. The signal observed in dRS-PAR4-expressing cells treated with 100 $\mu$M AYPGKF-$NH_2$ (red line) is also depicted. For clarity, traces for 0.3 and 1 $\mu$M AYPGKF-$NH_2$ in wt-PAR4-expressing cells, which lie on top of the dRS-PAR4 trace, are not shown.

cytometry-assisted cell sorting. In HEK-293 cells AYPGKF-$NH_2$ triggered concentration-dependent calcium signaling in wt-PAR4-YFP-expressing cells ($EC_{50}$ 10 $\mu$M). The dRS-PAR4-expressing cells did not generate a significant calcium signal (Fig. 1B and C), whereas in QC-PAR4-YFP-expressing cells AYPGKF-$NH_2$ acted as a partial agonist with responses seen at 100 and 300 $\mu$M concentrations, which were 50% of the maximum elicited in the wt-PAR4-YFP-expressing cells (Supplemental Fig. 1).

**MAPK Signaling in C-Terminal Mutant PAR4 Receptors.** Since in other studies we have observed that PARs can trigger MAPK signaling in the absence of calcium signaling (Ramachandran et al., 2009, 2011), we investigated MAPK activation in the HEK-293 cell lines expressing wt-PAR4-YFP or dRS-PAR4-YFP. Following activation of the cells with 100 $\mu$M AYPGKF-$NH_2$ for 10 minutes, significant elevation of p42/44 and p38 MAPK was detected using Proteome Profiler Human Phospho-MAPK Array Kit ARY002 (R&D Systems, Minneapolis, MN) for both wt and dRS-PAR4 (Supplemental Fig. 2A) In contrast, no activation-phosphorylation of RSK, GSK, JNK, and AKT was observed following PAR4 activation. Further, using a pepducin targeting the third intracellular loop (ICL3) of PAR4 (p4Pal10) (Covic et al., 2002), we were able to inhibit the AYPGKF-$NH_2$-triggered p38 MAPK activation (Supplemental Fig. 2B).

**Loss of $\beta$-Arrestin Interactions with dRS-PAR4 Receptors.** Since previous studies with other GPCRs have shown that MAPK activation can occur in the absence of G protein coupling through an arrestin-dependent mechanism (Luttrell and Gesty-Palmer, 2010), we investigated $\beta$-arrestin recruitment to wt-PAR4 and dRS-PAR4 using a BRET-based assay that monitored the interaction between YFP-tagged receptor and RLuc–$\beta$-arrestins. We found robust $\beta$-arrestin recruitment to wt-PAR4 in response to both thrombin and AYPGKF-$NH_2$ stimulation of cells (Fig. 2A). However, the dRS-PAR4-expressing cells did not recruit $\beta$-arrestin in response to either stimulus (Fig. 2A) whereas AYPGKF-$NH_2$ and thrombin triggered $\beta$-arrestin-1 and -2 recruitment to the QC-PAR4-YFP mutant receptor was not impaired (Supplemental Fig. 3, A and B). Together with the inhibition of p38 MAPK by an intracellular loop 3 targeted pepducin, we conclude that PAR4-dependent MAPK signaling is $\beta$-arrestin-independent and is dependent on PAR4 intracellular loop 3, and not C-terminus interaction with signaling effectors.

**Impaired Trafficking of dRS-PAR4 Receptors.** Following activation with AYPGKF-$NH_2$, wt-PAR4 internalized into vesicular structures as is expected for activated GPCRs, whereas the dRS-PAR4 mutant did not internalize (Fig. 2B), consistent with the observation that it did not recruit $\beta$-arrestins upon activation. Upon activation with AYPGKF-$NH_2$, the QC-PAR4 mutants also internalized like wt-PAR4 (Supplemental Fig. 3C). Thus, we conclude that the C-terminal eight-amino acid PAR4 motif that we have identified regulates calcium signaling, $\beta$-arrestin interaction with PAR4, and the internalization of activated receptors.

**Targeting Signaling Involving the PAR4 C-Terminal RAG8 Domain with Cell-Penetrating Peptides.** Having identified a key regulatory sequence in the PAR4 C-terminus, we investigated whether we could pharmacologically target this motif to modify receptor function using a cell-penetrating palmitoylated peptide (a pepducin) in keeping with the approach developed for other GPCRs (Tressel et al., 2011). Therefore, to target the C-terminus of PAR4 we synthesized a peptide with a sequence corresponding to the identified eight-amino acid motif in PAR4 (RAGLFQRS), coupled to an N-terminal palmitoyl moiety (RAG8) and C-terminal $NH_2$ (Fig. 3A). A control peptide had an identical architecture but with the reverse amino acid sequence (SRQFLGAR:SRQ8). We then investigated the ability of these peptides to regulate PAR4 function in various assays. At 10 $\mu$M, RAG8 attenuate calcium signaling triggered by 10, 30, and 100 $\mu$M of the PAR4 agonist peptide AYPGKF-$NH_2$ (Fig. 3B). Likewise, both $\beta$-arrestin-1 and $\beta$-arrestin-2 recruitment to AYPGKF-$NH_2$–activated PAR4 were significantly attenuated by 10 $\mu$M RAG8 (Fig. 3, C and D). RAG8 had no effect on the related GPCR, proteinase-activated receptor-2 recruitment of $\beta$-arrestin-1 and -2 (Supplemental Fig. 4).

**Targeting PAR4 to Regulate Platelet Function.** Previous work has shown that $\beta$-arrestin-2 supports PAR4 signaling in murine platelets, enabling platelet fibrinogen

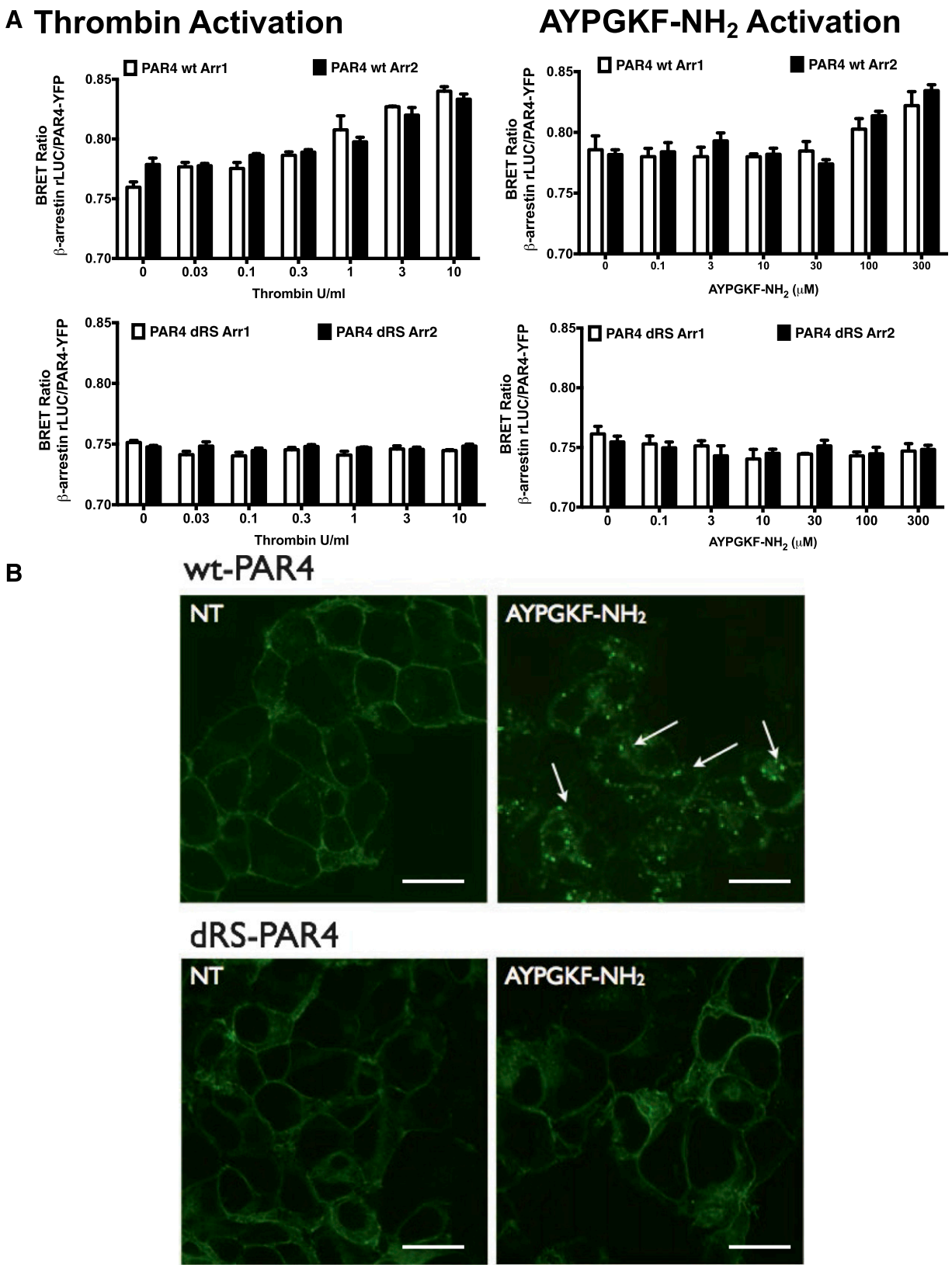


**Fig. 2.** PAR4 C-terminal domain is critical for PAR4-dependent $\beta$-arrestin interaction and trafficking. (A) HEK cells were cotransfected with RLuc-tagged $\beta$-arrestin-1 or -2 and wt-PAR4-YFP or dRS-PAR4-YFP. Thrombin or AYPGKF-$NH_2$–triggered recruitment of $\beta$-arrestin to the receptor was monitored. wt-PAR4-expressing cells show a concentration-dependent recruitment of $\beta$-arrestin that is abolished in the dRS-PAR4-expressing cell. Data are expressed as the mean ± S.E.M. from three independent experiments. (B) PAR4-YFP– or dRS-PAR4-YFP–expressing HEK cells were stimulated with the PAR4-activating peptide AYPGKF-$NH_2$ and internalization of the receptors was monitored by confocal microscopy. dRS-PAR4 failed to internalize following agonist treatment. Arrows indicate internalized receptor containing vesicles. The scale bar is 10 $\mu$m. Data are representative of the internalization seen in at least four independent experiments.

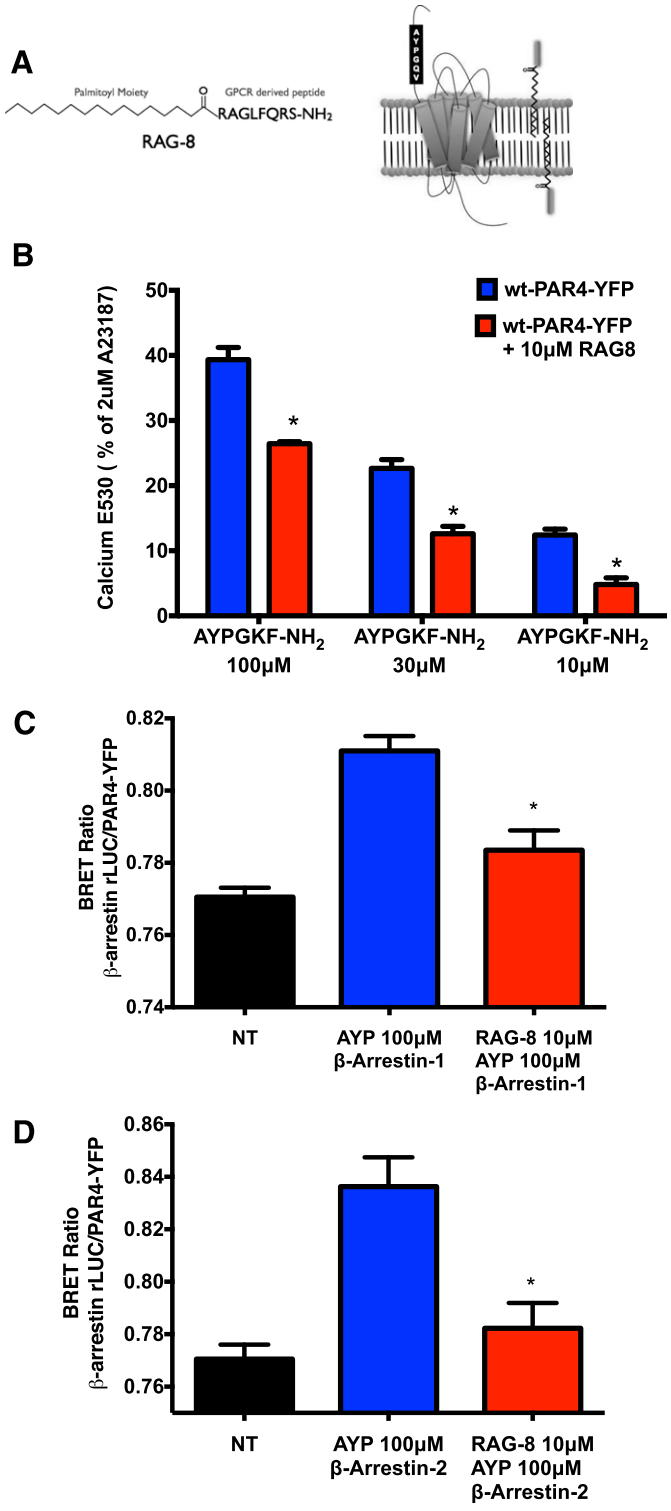


**Fig. 3.** RAG8 inhibits PAR4-dependent calcium signaling and β-arrestin recruitment. (A) Scheme depicting structure of RAG8 and proposed mechanism of action. (B) Pretreatment of cells with 10 μM RAG8 (20 minutes) PAR4-dependent calcium signaling. Data are expressed as the mean response relative to calcium ionophore A23187 from at least three separate experiments. An asterisk (*) indicates a significant difference ($P < 0.05$) in the RAG8-treated cells compared with the corresponding control cells and are the mean data from at least three independent experiments. Pretreatment of cells with 10 μM RAG8 (20 minutes) PAR4-dependent β-arrestin-1 (C) and β-arrestin-2 (D) recruitment to PAR4. An asterisk (*) indicates a significant difference ($P < 0.05$) in the RAG8-treated cells compared with the corresponding control cells and are the mean data ± S.E.M. from at least three independent experiments.

binding and thrombus formation (Li et al., 2011). We therefore hypothesized that by interdicting the PAR4-arrestin interaction with our RAG8 pepducin, we would affect PAR4-mediated platelet aggregation and clot consolidation. Indeed, in assays done with washed human platelets, RAG8 inhibited platelet aggregation stimulated by the PAR4 agonist peptide (AYPGKF-$NH_2$), but not by the PAR1 agonist peptide (TFLLR-$NH_2$) (Fig. 4A). Of note, RAG8 (Fig. 4B), but not the control peptide SRQ8 (not shown), also inhibited platelet aggregation triggered by thrombin.

Since AKT signaling is known to be involved in murine platelet activation (Woulfe et al., 2004), we investigated whether PAR4 activation could trigger AKT phosphorylation in human platelets and whether RAG8 modulates this process (Fig. 4C). In washed human platelets, the PAR4 agonist peptide and thrombin triggered an increase in phospho-AKT. RAG8 alone did not trigger a significant elevation of p-AKT, whereas RAG8 inhibited the AYPGKF-$NH_2$ and thrombin triggered elevation of AKT activation in a concentration-dependent manner (Fig. 4, C and D).

**Targeting PAR4 to Regulate Thrombus Formation In Vivo.** Because we were able to block platelet aggregation with our RAG8 pepducin in vitro, we next tested its ability to affect thrombosis in vivo in a rodent model in which platelet function is regulated by PAR4 in the absence of PAR1. We used spinning disc confocal microscopy to monitor murine thrombus formation following $FeCl_3$ blood vessel injury in the presence and absence of either RAG8 or the control peptide, SRQ8. In keeping with our results in vitro with washed platelets, we observed a significant inhibition of thrombosis at 15–30 minutes after $FeCl_3$ injury (Fig. 5, A and B) in RAG8-treated mice but not in SRQ8-treated animals. Upon analysis of the video recording of thrombus formation in real time after treatment with RAG8, we observed that at early time-points following $FeCl_3$ injury, the platelet thrombus does develop, but then very rapidly disintegrates and is washed away. This result suggested that RAG8 interferes with stabilization and consolidation of the platelet thrombus (Supplemental Video 1). This conclusion is supported by our observations using a tail-bleeding assay. We observed that in control mice, bleeding from the tail vein ceased completely at the 3-minute time point. However, in RAG8-treated mice, although bleeding also ceased at the 3-minute mark, blood flow then resumed, in some instances up to the 15-minute time-point when the experiment was concluded (Fig. 5C). This result indicated that the thrombus failed to stabilize.

## Discussion

Our main finding was that a specific motif in the C-terminus of PAR4 (RAGLFQRS) coordinately regulated calcium signaling and interactions of the receptor with β-arrestins-1 and -2. Yet, the receptor missing this domain was nonetheless able to trigger activation of MAPK. Further, by targeting this sequence with a cell-penetrating peptide (RAG8), we were able to block PAR4-dependent platelet activation in vitro and to attenuate clot stabilization in vivo without affecting signaling by PAR1. The impact of the RAG8 peptide on platelet aggregation and clot consolidation can be linked to its inhibition of Akt activation, which has been identified as a key arrestin-dependent signaling event for platelet activation (Woulfe et al., 2004; Li et al., 2011). Our work thus underscores the

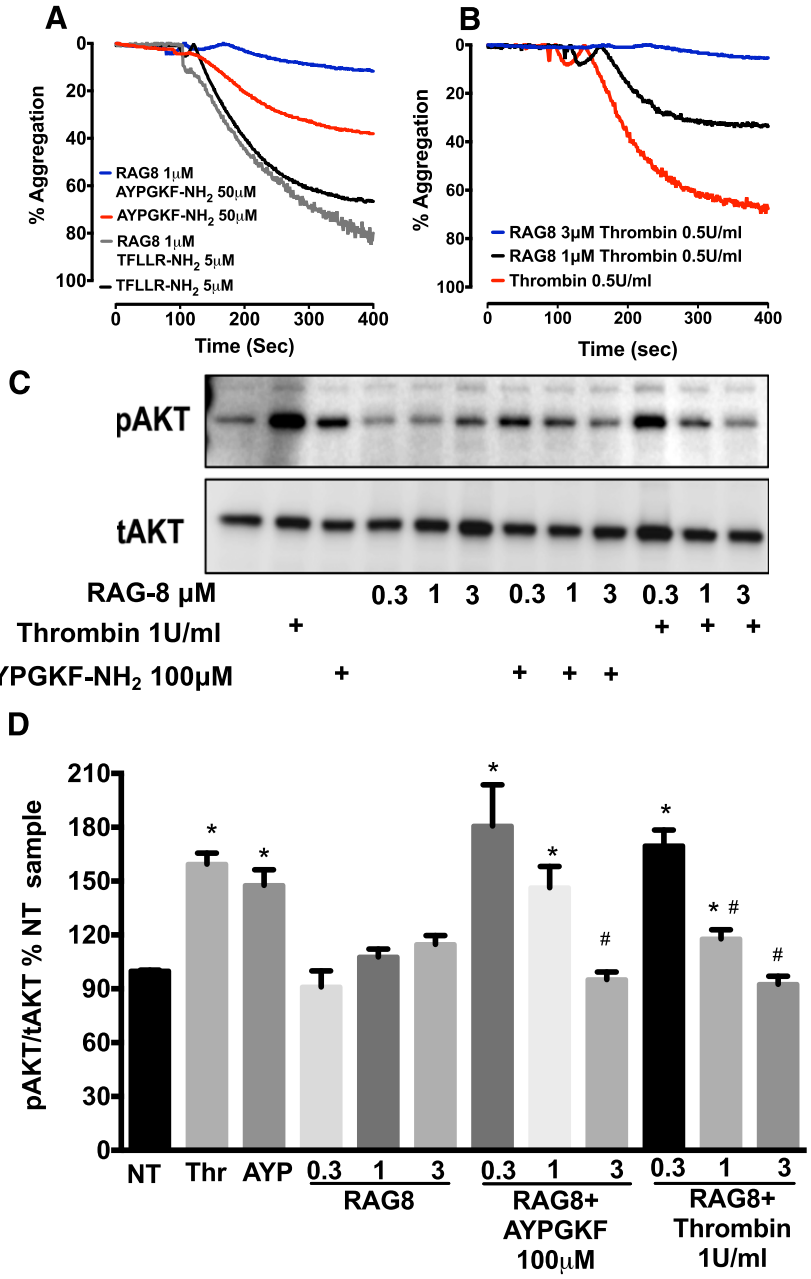


**Fig. 4.** Targeting the PAR4 intracellular motif to regulate human platelet function. Representative light transmission–aggregometry traces for platelet responses showing that (A) RAG8 inhibits platelet aggregation responses to PAR4 agonist peptide (AYPGKF-$NH_2$) but not the PAR1 agonist peptide (TFLLR-$NH_2$) (B) RAG8 inhibits thrombin-dependent platelet aggregation in platelets that express both PAR1 and PAR4 as the thrombin receptors. (C) Representative Western blot showing RAG8 inhibition of thrombin (1 units/ml) and AYPGKF-$NH_2$ (100 $\mu$M) stimulated AKT activation in human platelets. One-hundred microliters of a $3 \times 10^8$ cells/ml platelet cell suspension was treated with agonists for 10 minutes. Samples were pretreated with RAG8 for 20 minutes prior to agonist stimulation. (D) Densitometry analysis of phospho-AKT expression in human platelets normalized to total-AKT relative to the untreated samples (NT). Data are mean ± S.E.M. from three independent experiments. An asterisk (*) indicates significant difference ($P < 0.05$) from NT as calculated by an ordinary one-way analysis of variance with a Tukey's multiple comparisons test. $^{\#}P < 0.05$ (significant difference) from the corresponding non-RAG8–treated thrombin or AYPGKF-$NH_2$–treated sample.

utility of targeting PAR4 as an antithrombotic strategy, as an alternative to blocking platelet activation by PAR1. Our finding that deletion of a C-terminal motif disrupts $G\alpha_q$-dependent calcium signaling in addition to $\beta$-arrestin recruitment was unexpected since mutational and structural studies have shown that G protein-receptor interactions occur through contacts at the intracellular loops and transmembrane helices of GPCRs (Chung et al., 2011; Rasmussen et al., 2011; Venkatakrishnan et al., 2013). Although further work is required to understand the exact mechanisms, it is possible that the loss of signaling could come from a disruption of the network of receptor ionic and hydrogen-bond interactions that may form a so called "ionic lock" in the PAR4 carboxyl tail (Audet and Bouvier, 2012).

It is also interesting that dRS-PAR4 activation could still trigger MAPK signaling, suggesting that this occurs in a $\beta$-arrestin- and $G\alpha_q$-independent manner, probably through $G\alpha_{12/13}$ activation (Voss et al., 2007). In human platelets PAR4 does not interact with $G\alpha_i$ (Voss et al., 2007); however, PAR4 coupling to $G\alpha_i$ is reported in endothelial cells (Hirano et al., 2007). Using the P4pal10 pepducin that targets the ICL3 of PAR4 we were able to attenuate p38 MAPK signaling, pointing to ICL3 as the $G\alpha_{12/13}$- or $G\alpha_i$-interacting domain. Thus, our data point to the C-terminus of the PARs as motifs for developing pepducin-like receptor regulators, in addition to the intracellular loop sequences that have been used to date for the design of GPCR-inhibiting agents (O'Callaghan et al., 2012).

Our approach to blocking PAR4 activation complements the development of presumed orthosteric inhibitors of the receptor that are thought to target the tethered-ligand docking site, like YD-3 (Wu et al., 2000, 2002) and indoles substituted on

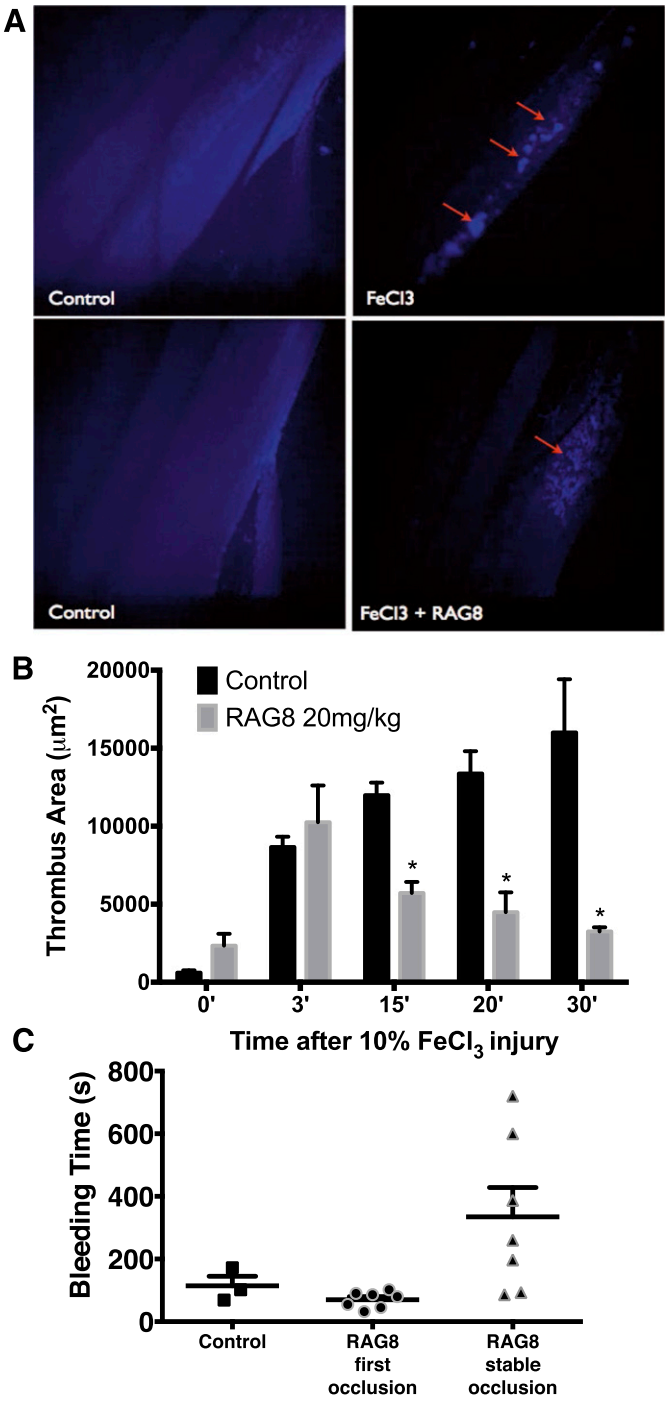


**Fig. 5.** RAG8 inhibits $FeCl_3$-triggered thrombosis in vivo. (A) Mice were injected intraperitoneally with RAG8 or the reverse control peptide SRQ8. Platelets were labeled with Alexa 647-CD49b antibody injected intravenously, the femoral artery and vein were exposed, and thrombosis was induced by placing a filter paper soaked in 10% $FeCl_3$. Images are taken over 30 minutes and image shown is at the 15-minute time-point. (B) The total area of the platelet thrombus was calculated over time. Data are the mean ± S.E.M. from at least three mice. An asterisk (*) indicates significant difference ($P < 0.05$) from corresponding control (C). Mice injected with RAG8 or SRQ8 (control) had tails cut 0.5 cm from the end of the tail, placed in a cuvette with warm saline, and time to cessation of bleeding monitored. Stable occlusion was determined to have occurred if the bleeding ceased for a full minute.

the basis of the YD-3 structure, such as ML354 (Young et al., 2013; Wen et al., 2014). The precise mechanism of antagonism of the indole-related compounds has not yet been determined. Further, whether the RAG8 sequence we have identified interacts directly with effectors like $G\alpha_q$ and the arrestins to modulate signaling or rather regulates the conformation of the C-terminal domain so as to change those interactions remains to be determined. Since we could not detect any inhibition of PAR1 or PAR2 signaling, RAG8 does appear to be a PAR4-specific inhibitor. The exact mechanism of action, however, remains to be elucidated. Nonetheless, the mechanisms whereby the indole-related compounds and the RAG8 pepducin block PAR4 activation will undoubtedly differ. Since PAR4 subserves many physiologic functions apart from regulating platelet reactivity, it will very probably be of value to block its actions in a pathway-selective manner, as per the RAG8 antagonist, rather than blocking all of its actions.

The mechanisms by which PAR4 stabilizes the platelet thrombus are not yet fully worked out, but PAR4 acts upstream of other factors that act to stabilize the platelet thrombus, including the activation of the P2Y12 receptors (Kim et al., 2002; Holinstat et al., 2006; Cornelissen et al., 2010; Li et al., 2011), and may serve as an important node for multiple thrombin-dependent responses in platelets. Thus, inhibition of PAR4 could prevent the formation of large occlusive thrombi, without preventing the formation of the small juxtamural thrombus that develops as a result of thrombin activation of PAR1. This selective inhibition of PAR4 that enables perivascular homeostasis may be of particular relevance in individuals with a PAR4 mutation that renders their platelets more susceptible to PAR4 activation (Edelstein et al., 2013, 2014).

In conclusion, we have uncovered a novel molecular determinant of PAR4 signaling involving its C-terminal domain and have developed a cell-penetrating peptide constructed on the basis of this sequence that blocks PAR4-stimulated platelet activation and thrombus consolidation. This inhibition of PAR4 provides an attractive alternative to blocking PAR1 for dealing with vascular occlusive disease. We believe that this signaling mechanism may also be a therapeutic target in other settings where PAR4 can be involved and propose that the use of RAG8 could also be of benefit in pathologies such as pain and inflammatory disease (McDougall et al., 2009; Mao et al., 2010) in which PAR4 is thought to play an important role.

#### Acknowledgments

The authors thank Michael Dicay for help with the platelet aggregation assays. This work was supported by the Snyder Mouse Phenomics Resources Laboratory and Live Cell Imaging Facility, both of which were funded by the Snyder Institute for Chronic Diseases at the University of Calgary.

#### Authorship Contributions

*Participated in research design:* Ramachandran, Bouvier, Hollenberg.

*Conducted experiments:* Ramachandran, Mihara, Thibeault, Vanderboor, Petri, Saifeddine.

*Performed data analysis:* Ramachandran, Mihara, Petri.

*Wrote or contributed to the writing of the manuscript:* Ramachandran, Petri, Bouvier, Hollenberg.

#### References

Aisiku O, Peters CG, De Ceunynck K, Ghosh CC, Dilks JR, Fustolo-Gunnink SF, Huang M, Dockendorff C, Parikh SM, and Flaumenhaft R (2015) Parmodulins inhibit thrombus formation without inducing endothelial injury caused by vorapaxar. *Blood* **125**:1976–1985.

Andrade-Gordon P, Maryanoff BE, Derian CK, Zhang HC, Addo MF, Darrow AL, Eckardt AJ, Hoekstra WJ, McComsey DF, Oksenberg D, et al. (1999) Design, synthesis, and biological characterization of a peptide-mimetic antagonist for a tethered-ligand receptor. *Proc Natl Acad Sci USA* **96**:12257–12262.

Audet M and Bouvier M (2012) Restructuring G-protein- coupled receptor activation. *Cell* **151**:14–23.

Bae JS and Rezaie AR (2008) Protease activated receptor 1 (PAR-1) activation by thrombin is protective in human pulmonary artery endothelial cells if endothelial protein C receptor is occupied by its natural ligand. *Thromb Haemost* **100**:101–109.

Baker NC, Lipinski MJ, Lhermusier T, and Waksman R (2014) Overview of the 2014 Food and Drug Administration Cardiovascular and Renal Drugs Advisory Committee meeting about vorapaxar. *Circulation* **130**:1287–1294.

Bernatowicz MS, Klimas CE, Hartl KS, Peluso M, Allegretto NJ, and Seiler SM (1996) Development of potent thrombin receptor antagonist peptides. *J Med Chem* **39**:4879–4887.

Chackalamannil S, Wang Y, Greenlee WJ, Hu Z, Xia Y, Ahn HS, Boykow G, Hsieh Y, Palamanda J, Agans-Fantuzzi J, et al. (2008) Discovery of a novel, orally active himbacine-based thrombin receptor antagonist (SCH 530348) with potent antiplatelet activity. *J Med Chem* **51**:3061–3064.

Chackalamannil S, Xia Y, Greenlee WJ, Clasby M, Doller D, Tsai H, Asberom T, Czarniecki M, Ahn HS, Boykow G, et al. (2005) Discovery of potent orally active thrombin receptor (protease activated receptor 1) antagonists as novel antithrombotic agents. *J Med Chem* **48**:5884–5887.

Chung KY, Rasmussen SG, Liu T, Li S, DeVree BT, Chae PS, Calinski D, Kobilka BK, Woods, JrVL, and Sunahara RK (2011) Conformational changes in the G protein Gs induced by the β2 adrenergic receptor. *Nature* **477**:611–615.

Cornelissen I, Palmer D, David T, Wilsbacher L, Concengco C, Conley P, Pandey A, and Coughlin SR (2010) Roles and interactions among protease-activated receptors and P2ry12 in hemostasis and thrombosis. *Proc Natl Acad Sci USA* **107**: 18605–18610.

Coughlin SR (2000) Thrombin signalling and protease-activated receptors. *Nature* **407**:258–264.

Covic L, Misra M, Badar J, Singh C, and Kuliopulos A (2002) Pepducin-based intervention of thrombin-receptor signaling and systemic platelet activation. *Nat Med* **8**:1161–1165.

Derian CK, Damiano BP, Addo MF, Darrow AL, D'Andrea MR, Nedelman M, Zhang HC, Maryanoff BE, and Andrade-Gordon P (2003) Blockade of the thrombin receptor protease-activated receptor-1 with a small-molecule antagonist prevents thrombus formation and vascular occlusion in nonhuman primates. *J Pharmacol Exp Ther* **304**:855–861.

Dowal L, Sim DS, Dilks JR, Blair P, Beaudry S, Denker BM, Koukos G, Kuliopulos A, and Flaumenhaft R (2011) Identification of an antithrombotic allosteric modulator that acts through helix 8 of PAR1. *Proc Natl Acad Sci USA* **108**:2951–2956.

Edelstein LC, Simon LM, Lindsay CR, Kong X, Teruel-Montoya R, Tourdot BE, Chen ES, Ma L, Coughlin S, Nieman M, et al. (2014) Common variants in the human platelet PAR4 thrombin receptor alter platelet function and differ by race. *Blood* **124**:3450–3458.

Edelstein LC, Simon LM, Montoya RT, Holinstat M, Chen ES, Bergeron A, Kong X, Nagalla S, Mohandas N, Cohen DE, et al. (2013) Racial differences in human platelet PAR4 reactivity reflect expression of PCTP and miR-376c. *Nat Med* **19**: 1609–1616.

Feistritzer C, Schuepbach RA, Mosnier LO, Bush LA, Di Cera E, Griffin JH, and Riewald M (2006) Protective signaling by activated protein C is mechanistically linked to protein C activation on endothelial cells. *J Biol Chem* **281**: 20077–20084.

Goto S, Yamaguchi T, Ikeda Y, Kato K, Yamaguchi H, and Jensen P (2010) Safety and exploratory efficacy of the novel thrombin receptor (PAR-1) antagonist SCH530348 for non-ST-segment elevation acute coronary syndrome. *J Atheroscler Thromb* **17**:156–164.

Hirano K, Nomoto N, Hirano M, Momota F, Hanada A, and Kanaide H (2007) Distinct Ca2+ requirement for NO production between proteinase-activated receptor 1 and 4 (PAR1 and PAR4) in vascular endothelial cells. *J Pharmacol Exp Ther* **322**: 668–677.

Holinstat M, Voss B, Bilodeau ML, McLaughlin JN, Cleator J, and Hamm HE (2006) PAR4, but not PAR1, signals human platelet aggregation via Ca2+ mobilization and synergistic P2Y12 receptor activation. *J Biol Chem* **281**:26665–26674.

Kim S, Foster C, Lecchi A, Quinton TM, Prosser DM, Jin J, Cattaneo M, and Kunapuli SP (2002) Protease-activated receptors 1 and 4 do not stimulate G(i) signaling pathways in the absence of secreted ADP and cause human platelet aggregation independently of G(i) signaling. *Blood* **99**:3629–3636.

Li D, D'Angelo L, Chavez M, and Woulfe DS (2011) Arrestin-2 differentially regulates PAR4 and ADP receptor signaling in platelets. *J Biol Chem* **286**:3805–3814.

Luttrell LM and Gesty-Palmer D (2010) Beyond desensitization: physiological relevance of arrestin-dependent signaling. *Pharmacol Rev* **62**:305–330.

Mao Y, Zhang M, Tuma RF, and Kunapuli SP (2010) Deficiency of PAR4 attenuates cerebral ischemia/reperfusion injury in mice. *J Cereb Blood Flow Metab* **30**:1044–1052.

McDougall JJ, Zhang C, Cellars L, Joubert E, Dixon CM, and Vergnolle N (2009) Triggering of proteinase-activated receptor 4 leads to joint pain and inflammation in mice. *Arthritis Rheum* **60**:728–737.

McKee SA, Sane DC, and Deliargyris EN (2002) Aspirin resistance in cardiovascular disease: a review of prevalence, mechanisms, and clinical significance. *Thromb Haemost* **88**:711–715.

Mihara K, Ramachandran R, Renaux B, Saifeddine M, and Hollenberg MD (2013) Neutrophil elastase and proteinase-3 trigger G protein-biased signaling through proteinase-activated receptor-1 (PAR1). *J Biol Chem* **288**:32979–32990.

Morrow DA, Braunwald E, Bonaca MP, Ameriso SF, Dalby AJ, Fish MP, Fox KA, Lipka LJ, Liu X, Nicolau JC, et al.; TRA 2P–TIMI 50 Steering Committee and Investigators (2012) Vorapaxar in the secondary prevention of atherothrombotic events. *N Engl J Med* **366**:1404–1413.

Morrow DA, Scirica BM, Fox KA, Berman G, Strony J, Veltri E, Bonaca MP, Fish P, McCabe CH, and Braunwald E (2009) Evaluation of a novel antiplatelet agent for secondary prevention in patients with a history of atherosclerotic disease: design and rationale for the Thrombin-Receptor Antagonist in Secondary Prevention of Atherothrombotic Ischemic Events (TRA 2 degrees P)-TIMI 50 trial. *Am Heart J* **158**:335–341.e3 DOI: 10.1016/j.ahj.2009.06.027.

O'Callaghan K, Kuliopulos A, and Covic L (2012) Turning receptors on and off with intracellular pepducins: new insights into G-protein-coupled receptor drug development. *J Biol Chem* **287**:12787–12796.

Qanbar R and Bouvier M (2003) Role of palmitoylation/depalmitoylation reactions in G-protein-coupled receptor function. *Pharmacol Ther* **97**:1–33.

Ramachandran R (2012) Developing PAR1 antagonists: minding the endothelial gap. *Discov Med* **13**:425–431.

Ramachandran R, Mihara K, Chung H, Renaux B, Lau CS, Muruve DA, DeFea KA, Bouvier M, and Hollenberg MD (2011) Neutrophil elastase acts as a biased agonist for proteinase-activated receptor-2 (PAR2). *J Biol Chem* **286**:24638–24648.

Ramachandran R, Mihara K, Mathur M, Rochdi MD, Bouvier M, Defea K, and Hollenberg MD (2009) Agonist-biased signaling via proteinase activated receptor-2: differential activation of calcium and mitogen-activated protein kinase pathways. *Mol Pharmacol* **76**:791–801.

Rasmussen SG, DeVree BT, Zou Y, Kruse AC, Chung KY, Kobilka TS, Thian FS, Chae PS, Pardon E, Calinski D, et al. (2011) Crystal structure of the β2 adrenergic receptor-Gs protein complex. *Nature* **477**:549–555.

Riewald M and Ruf W (2005) Protease-activated receptor-1 signaling by activated protein C in cytokine-perturbed endothelial cells is distinct from thrombin signaling. *J Biol Chem* **280**:19808–19814.

Schuepbach RA, Feistritzer C, Fernández JA, Griffin JH, and Riewald M (2009) Protection of vascular barrier integrity by activated protein C in murine models depends on protease-activated receptor-1. *Thromb Haemost* **101**:724–733.

Schuepbach RA, Madon J, Ender M, Galli P, and Riewald M (2012) Protease-activated receptor-1 cleaved at R46 mediates cytoprotective effects. *J Thromb Haemost* **10**:1675–1684.

Serebruany VL, Kogushi M, Dastros-Pitei D, Flather M, and Bhatt DL (2009) The in-vitro effects of E5555, a protease-activated receptor (PAR)-1 antagonist, on platelet biomarkers in healthy volunteers and patients with coronary artery disease. *Thromb Haemost* **102**:111–119.

Tressel SL, Koukos G, Tchernychev B, Jacques SL, Covic L, and Kuliopulos A (2011) Pharmacology, biodistribution, and efficacy of GPCR-based pepducins in disease models. *Methods Mol Biol* **683**:259–275.

Tricoci P, Huang Z, Held C, Moliterno DJ, Armstrong PW, Van de Werf F, White HD, Aylward PE, Wallentin L, Chen E, et al.; TRACER Investigators (2012) Thrombin-receptor antagonist vorapaxar in acute coronary syndromes. *N Engl J Med* **366**: 20–33.

Venkatakrishnan AJ, Deupi X, Lebon G, Tate CG, Schertler GF, and Babu MM (2013) Molecular signatures of G-protein-coupled receptors. *Nature* **494**:185–194.

Voss B, McLaughlin JN, Holinstat M, Zent R, and Hamm HE (2007) PAR1, but not PAR4, activates human platelets through a Gi/o/phosphoinositide-3 kinase signaling axis. *Mol Pharmacol* **71**:1399–1406.

Wen W, Young SE, Duvernay MT, Schulte ML, Nance KD, Melancon BJ, Engers J, Locuson, 2ndCW, Wood MR, Daniels JS, et al. (2014) Substituted indoles as selective protease activated receptor 4 (PAR-4) antagonists: Discovery and SAR of ML354. *Bioorg Med Chem Lett* **24**:4708–4713.

Wiviott SD and Antman EM (2004) Clopidogrel resistance: a new chapter in a fast-moving story. *Circulation* **109**:3064–3067.

Woulfe D, Jiang H, Morgans A, Monks R, Birnbaum M, and Brass LF (2004) Defects in secretion, aggregation, and thrombus formation in platelets from mice lacking Akt2. *J Clin Invest* **113**:441–450.

Wu CC, Huang SW, Hwang TL, Kuo SC, Lee FY, and Teng CM (2000) YD-3, a novel inhibitor of protease-induced platelet activation. *Br J Pharmacol* **130**:1289–1296.

Wu CC, Hwang TL, Liao CH, Kuo SC, Lee FY, Lee CY, and Teng CM (2002) Selective inhibition of protease-activated receptor 4-dependent platelet activation by YD-3. *Thromb Haemost* **87**:1026–1033.

Xu WF, Andersen H, Whitmore TE, Presnell SR, Yee DP, Ching A, Gilbert T, Davie EW, and Foster DC (1998) Cloning and characterization of human protease-activated receptor 4. *Proc Natl Acad Sci USA* **95**:6642–6646.

Young SE, Duvernay MT, Schulte ML, Lindsley CW, and Hamm HE (2013) Synthesis of indole derived protease-activated receptor 4 antagonists and characterization in human platelets. *PLoS One* **8**:e65528.

**Address correspondence to:** Dr. Rithwik Ramachandran, Department of Physiology and Pharmacology, Schulich Medicine and Dentistry, University of Western Ontario, MSB 270, 1151 Richmond St., London, Ontario, N6A 5C1. E-mail: rramach@uwo.ca